the FEBS Journal

Physical properties and surface activity of surfactant-like membranes containing the cationic and hydrophobic peptide KL_4

Alejandra Sáenz[1,*], Olga Cañadas[1,*], Luís A. Bagatolli[2], Mark E. Johnson[3] and Cristina Casals[1]

1 Department of Biochemistry and Molecular Biology I, Complutense University of Madrid, Spain
2 MEMPHYS-Center for Biomembrane Physics, Department of Biochemistry and Molecular Biology, University of Southern Denmark, Odense, Denmark
3 Discovery Laboratories, Mountain View, CA, USA

Keywords
differential scanning calorimetry; DPH fluorescence; GUV; lung surfactant; surface adsorption

Correspondence
C. Casals, Department of Biochemistry and Molecular Biology I, Faculty of Biology, Complutense University of Madrid, 28040 Madrid, Spain
Fax: +34 91 3944672
Tel: +34 91 3944261
E-mail: ccasalsc@bio.ucm.es

*These authors contributed equally to this study

(Received 5 March 2006, revised 31 March 2006, accepted 3 April 2006)

doi:10.1111/j.1742-4658.2006.05258.x

Surfactant-like membranes containing the 21-residue peptide KLLLL-KLLLLKLLLLKLLLLK (KL_4), have been clinically tested as a therapeutic agent for respiratory distress syndrome in premature infants. The aims of this study were to investigate the interactions between the KL_4 peptide and lipid bilayers, and the role of both the lipid composition and KL_4 structure on the surface adsorption activity of KL_4-containing membranes. We used bilayers of three-component systems [1,2-dipalmitoyl-phosphatidylcholine/1-palmitoyl-2-oleoyl-phosphatidylglycerol/palmitic acid (DPPC/POPG/PA) and DPPC/1-palmitoyl-2-oleoyl-phosphatidylcholine (POPC)/PA] and binary lipid mixtures of DPPC/POPG and DPPC/PA to examine the specific interaction of KL_4 with POPG and PA. We found that, at low peptide concentrations, KL_4 adopted a predominantly α-helical secondary structure in POPG- or POPC-containing membranes, and a β-sheet structure in DPPC/PA vesicles. As the concentration of the peptide increased, KL_4 interconverted to a β-sheet structure in DPPC/POPG/PA or DPPC/POPC/PA vesicles. Ca^{2+} favored α↔β interconversion. This conformational flexibility of KL_4 did not influence the surface adsorption activity of KL_4-containing vesicles. KL_4 showed a concentration-dependent ordering effect on POPG- and POPC-containing membranes, which could be linked to its surface activity. In addition, we found that the physical state of the membrane had a critical role in the surface adsorption process. Our results indicate that the most rapid surface adsorption takes place with vesicles showing well-defined solid/fluid phase co-existence at temperatures below their gel to fluid phase transition temperature, such as those of DPPC/POPG/PA and DPPC/POPC/PA. In contrast, more fluid (DPPC/POPG) or excessively rigid (DPPC/PA) KL_4-containing membranes fail in their ability to adsorb rapidly onto and spread at the air–water interface.

Abbreviations
Bodipy-PC, 2-(4,4-difluoro-5,7-dimethyl-4-bora-3α,4α-diaza-*s*-indacene-3-pentanoyl)-1-hexadecanoyl-*sn*-glycero-3-phosphocholine; DPH, 1,6-diphenyl-1,3,5-hexatriene; DPPC, 1,2-dipalmitoyl-phosphatidylcholine; DSC, differential scanning calorimetry; GUV, giant unilamellar vesicle; PA, palmitic acid; PC, phosphatidylcholine; POPC, 1-palmitoyl-2-oleoyl-phosphatidylcholine; POPG, 1-palmitoyl-2-oleoyl-phosphatidylglycerol; RDS, respiratory distress syndrome; SP-B, surfactant protein B; SP-C, surfactant protein C; T_m, gel to fluid phase transition temperature.

The human lung has an alveolar surface of 50–100 m^2, which is completely covered with a lipid–protein complex called pulmonary surfactant [1]. The primary role of this material is to prevent collapse of the alveoli during end-expiration, preclude blood fluid transudation into the alveolar spaces, participate in lung defense against inhaled pathogens and toxins, and modulate the function of respiratory inflammatory cells [1–4]. The alteration or deficiency of this system leads to respiratory distress.

The main phospholipid constituent of pulmonary surfactant is phosphatidylcholine (PC), especially 1,2-dipalmitoyl-phosphatidylcholine (DPPC) [5]. Phosphatidylglycerol represents a major unsaturated anionic component [5]. Four surfactant proteins (A, B, C and D) have been isolated. Surfactant protein B (SP-B) is a small hydrophobic protein that is essential for lung function and pulmonary homeostasis after birth. The genetic absence of SP-B in both humans and mice results in a lack of alveolar expansion and a lethal lack of pulmonary function [3]. In contrast, the genetic absence of surfactant protein C (SP-C), another small hydrophobic peptide, results in the normal expansion of alveoli and pulmonary function, although it is associated with interstitial lung diseases over time [3]. These hydrophobic proteins enhance the spreading, adsorption and stability of surfactant lipids required for the reduction of surface tension in the alveolus [3]. On the other hand, surfactant protein A (SP-A) and surfactant protein D (SP-D) are oligomeric water-soluble proteins that modulate pulmonary innate immunity [4].

Neonatal respiratory distress syndrome (RDS) is caused by lung immaturity with a deficiency of surfactant in the alveolar spaces. RDS is a major cause of morbidity and mortality in preterm babies. Experience from replacement therapy on RDS indicates that SP-B and SP-C are essential constituents of exogenous surfactants [6]. Given that natural surfactants from animal sources raise microbiological, immunological, economic and purity concerns, many efforts have been made to develop synthetic surfactant replacement formulations, which involve a combination of synthetic lipids with either synthetic or recombinant peptides [7]. Synthetic surfactant peptides, based on patterns of structure or charge found in human SP-B or SP-C, appear to mimic some of the structural and functional properties of the native proteins and thus may offer a useful basis for the design of agents for therapeutic intervention [7]. Studies of different fragments and mutants of SP-B suggest that the function-related structural and compositional characteristics of SP-B are its positive charges with intermittent hydrophobic domains [8,9]. Cochrane & Revak [10] designed a 21-residue peptide (KLLLLKLLLLKLLLLKLLLLK, where 'K' and 'L' represent the amino acids lysine and leucine, respectively), named KL_4, to mimic the positive charge and hydrophobic residue distribution of SP-B. A synthetic lung surfactant formulation was developed based upon KL_4 (Surfaxin®; lucinactant), which is composed of DPPC, 1-palmitoyl-2-oleoyl-phosphatidylglycerol (POPG), palmitic acid (PA) and KL_4 at weight ratios of 28 : 9.3 : 5.0 : 1.0 and has been found to be very effective in the clinical trials of human RDS [11,12]. This KL_4 concentration corresponds to 0.57 mol% and 2.3 wt%. Of great interest is the fact that airway lavage performed with diluted KL_4 surfactant improves the lung function in experimental and clinical meconium aspiration syndrome [13] and in patients with acute respiratory distress syndrome (ARDS) [14].

The surface activity of KL_4 peptide incorporated in bilayers and monolayers is well recognized [10,15–18]. However, little is known about the interactions between KL_4 peptide and lipid bilayers, and their dependence on calcium. Therefore, the objectives of this study were to analyze (a) the effect of KL_4 on the physical properties of membranes, in the absence and presence of Ca^{2+}, using fluorescence anisotropy of 1,6-diphenyl-1,3,5-hexatriene (DPH), differential scanning calorimetry (DSC) and fluorescence confocal microscopy of giant unilamellar vesicles (GUVs), (b) the effect of the lipid composition on KL_4 structure, in the absence and presence of Ca^{2+}, using CD and (c) the role of the lipid composition and peptide structure on surface adsorption activity.

Results and Discussion

This study was performed with four different types of vesicles: DPPC/POPG (27 : 9, w/w), DPPC/POPG/PA (28 : 9.4 : 5.1, w/w/w), DPPC/1-palmitoyl-2-oleoyl-phosphatidylcholine (POPC)/PA (28 : 9.4 : 5.1, w/w/w), and DPPC/PA (28 : 5.1, w/w) with and without different amounts of the cationic and hydrophobic peptide, KL_4. The composition of bilayers of three-component systems was chosen according to the following criteria (a) a high DPPC content, which is the main phospholipid constituent of pulmonary surfactant, (b) the presence of unsaturated phospholipids (either POPG or POPC, which constitute up to 10% and 20%, respectively, in human pulmonary surfactant) [5] and (c) the presence of PA, which is a common additive in replacement surfactants because it increases the surface activity of these formulations [18,19], except that of a synthetic surfactant based on a poly Leu SP-C analog [20]. In addition, binary lipid mixtures (DPPC/POPG and DPPC/PA) were used to

specifically examine the interaction of KL_4 with POPG and PA as well as the effect of these lipids on the physical properties of the membrane.

Effect of KL_4 on the lipid order of surfactant-like membranes

To evaluate KL_4 effects on the lipid order of surfactant-like liposomes, the steady-state fluorescence emission anisotropy, *r*, of DPH incorporated in DPPC/POPG, DPPC/POPG/PA, DPPC/POPC/PA and DPPC/PA vesicles was measured as a function of KL_4 concentration at 37 °C (Fig. 1). In the absence of the peptide, DPH anisotropy values in DPPC/POPG vesicles were strikingly smaller than those obtained in membranes of either DPPC/POPC/PA or DPPC/POPG/PA. These results might be indicative of greater acyl chain order in PA-containing vesicles, allowing slower DPH rotational diffusion and hence higher DPH anisotropy values. For DPPC/PA at 37 °C, the steady-state anisotropy of DPH in the absence of KL_4 was ≈ 0.35, which is within the range of the observable DPH anisotropy in phospholipid vesicles in the gel phase (0.30–0.35) [21]. The incorporation of increasing KL_4 concentrations in DPPC/PA liposomes resulted in insignificant changes in DPH anisotropy (Fig. 1, white circles). In contrast, increasing the KL_4 concentration in DPPC/POPG (black circles), DPPC/POPG/PA (black squares), and DPPC/POPC/PA (white squares) vesicles resulted in a small, but significant, increase in anisotropy.

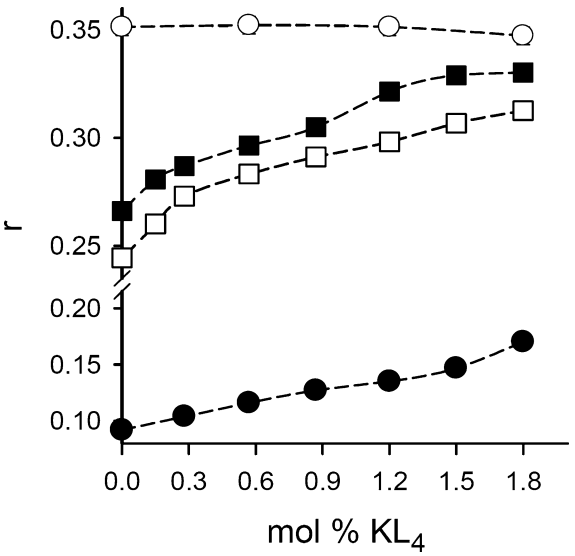

Fig. 1. Steady-state emission anisotropy of 1,6-diphenyl-1,3,5-hexatriene (DPH) incorporated in DPPC/POPG (●), DPPC/POPG/PA (■), DPPC/POPC/PA (□) or DPPC/PA (○) vesicles containing different concentrations of KL_4 at 37 °C. [Excitation wavelength (λ_x) = 360 nm; emission wavelength (λ_m) = 430 nm.] Values represent the mean ± SD of three experiments. DPPC, 1,2-dipalmitoyl-phosphatidylcholine; PA, palmitic acid; POPC, 1-palmitoyl-2-oleoyl-phosphatidylcholine; POPG, 1-palmitoyl-2-oleoyl-phosphatidylglycerol.

To establish whether the increase in DPH steady-state anisotropy in these vesicles caused by KL_4 was the result of a greater molecular order of lipids surrounding DPH and a consequent slowing in DPH rotational diffusion, or of changes in DPH fluorescence lifetime, and, hence, changes in DPH steady-state fluorescence intensity [22], we determined the effect of different amounts of KL_4 on the fluorescence emission spectra of DPH in DPPC/POPG, DPPC/POPG/PA and DPPC/POPC/PA vesicles upon excitation at 340 nm, at 37 °C. The lack of changes, within experimental error, in the fluorescence emission of DPH with increasing amounts of peptide (data not shown), allows us to infer that KL_4 enhances the lipid order of DPPC/POPG, DPPC/POPG/PA and DPPC/POPC/PA membranes. These results are consistent with the ordering effect of SP-B and related peptides on the polar surface of DPPC/PG vesicles [23,24].

Thermotropic properties of KL_4-containing membranes

Next, we used the nonperturbing technique of DSC to study the effect of KL_4 on the thermotropic properties of surfactant-like membranes (Fig. 2). In the absence of the peptide, DPPC/POPG/PA, DPPC/POPC/PA and DPPC/PA multilamellar vesicles showed endotherms with a gel to fluid phase transition temperature (T_m) of 48.5, 46.1 and 52.2 °C, respectively. In the absence of PA, the T_m of DPPC/POPG, DPPC/POPC and DPPC multilamellar vesicles shifted to lower temperatures (32.5, 35.3 and 41.5 °C, respectively), indicating that the fatty acid markedly raised the main transition temperature of these types of vesicles. This is consistent with the PA ordering effect in DPPC/POPG/PA vesicles determined from DPH anisotropy measurements.

DSC measurements indicated that a relatively small amount of KL_4 (0.28 mol%) exerted a significant effect on the thermotropic behavior of DPPC/POPG, DPPC/POPG/PA and DPPC/POPC/PA vesicles. KL_4 shifted the T_m of those vesicles somewhat upward (from 32.5 to 34 °C for DPPC/POPG, from 48.5 to 49.0 °C for DPPC/POPG/PA, and from 46.1 to 48.3 °C for DPPC/POPC/PA) and narrowed the phase transition (Fig. 2). The slight increase in T_m is in agreement with the KL_4 ordering effect determined from DPH anisotropy measurements. The KL_4-induced narrowing of the phase transition might be a consequence of the interaction of KL_4 with POPG

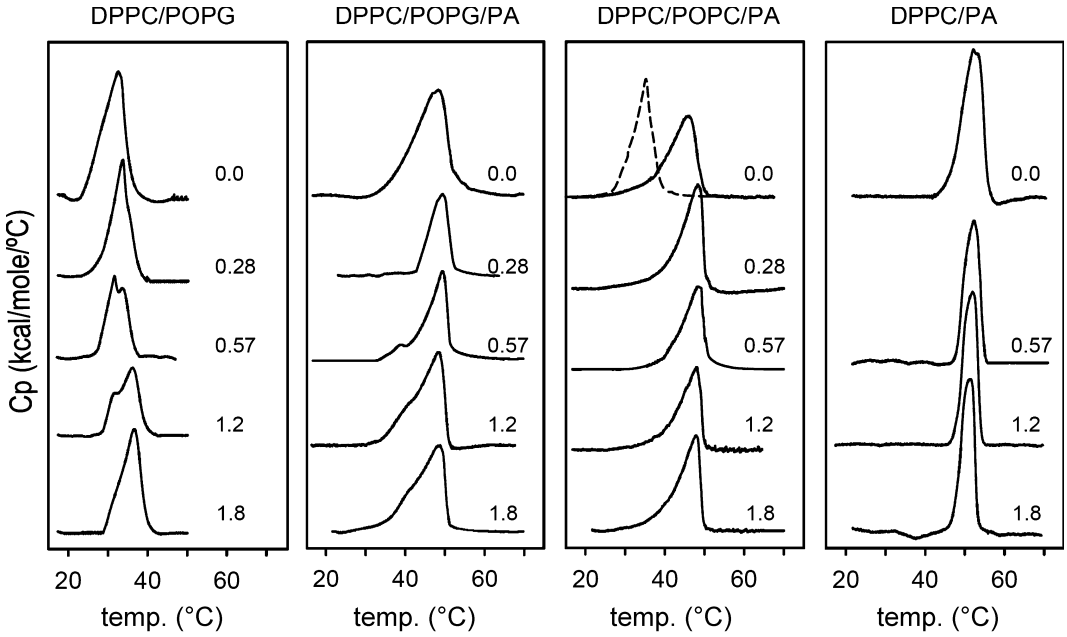

Fig. 2. Differential scanning calorimetry (DSC) heating scans of DPPC/POPG, DPPC/POPG/PA, DPPC/POPC/PA and DPPC/PA multilamellar vesicles (1 mM) in the absence and presence of different concentrations of KL_4. The mole percentage of KL_4 is indicated on each thermogram. The dashed line represents the thermogram of DPPC/POPC multilamellar vesicles (1 mM). Calorimetric scans were performed at a rate of 0.5 °C·min^{-1}. DPPC, 1,2-dipalmitoyl-phosphatidylcholine; PA, palmitic acid; POPC, 1-palmitoyl-2-oleoyl-phosphatidylcholine; POPG, 1-palmitoyl-2-oleoyl-phosphatidylglycerol.

and/or PA [15], which may decrease the miscibility between these lipids and DPPC. A high level of miscibility between DPPC and POPG in bilayers or monolayers has been reported [15,25] and can be visualized for GUVs of DPPC/POPG and DPPC/POPC shown in this study.

In addition, DSC thermograms indicated that, at peptide mole percentages higher than 0.28, the thermal transition of POPG-containing vesicles was characterized by a double peak. This double peak was not observed in DPPC/POPC/PA or DPPC/PA vesicles, indicating that it must be generated by electrostatic interactions between the positively charged lysine residues of KL_4 and the anionic headgroup of POPG. On the other hand, when KL_4 (0.57–1.8 mol%) was incorporated into DPPC/PA vesicles, the main transition temperature did not change. However, KL_4 induced narrowing of the phase transition, which is a measure of stabilization of DPPC-rich assemblies.

Effect of calcium on the thermotropic properties of KL_4-containing membranes

In order to simplify the nature of the thermal transition of these vesicles and allow a less ambiguous assessment of the effect of KL_4, calcium was omitted in the DSC experiments reported above. However, calcium ions affect the structure and biophysical activity of lung surfactant [1,2]. Moreover, calcium is present in the alveolar fluid at a concentration of $\approx$1.8 mM [26]. To determine whether the presence of calcium modifies the effects of KL_4 on the thermotropic behavior of surfactant-like vesicles, experiments in the presence of physiological concentrations of calcium were performed. Figure 3 shows that the addition of 1.8 mM $CaCl_2$ to DPPC/POPG vesicles, containing 0.57 mol% KL_4, slightly increased the phase transition temperature (Fig. 3A). However, the presence of calcium markedly decreased the main transition temperature of PA-containing membranes with 0.57 mol% KL_4. Thus, in the presence of Ca^{2+}, the T_m values of KL_4-containing membranes shifted from 52.2 to 49.5 °C for DPPC/PA (Fig. 3B), from 46.1 to 41.5 °C for DPPC/POPC/PA (Fig. 3C), and from 48.5 to 39.5 °C for DPPC/POPG/PA (Fig. 3D). These results suggest that the calcium-dependent T_m decrease observed only in PA-containing membranes might be caused by specific interactions between the fatty acid and calcium ions, which seem to result in the partial extraction of PA from the bilayer. Further addition of calcium, up to 5 mM, did not appreciably modify the thermotropic properties of DPPC/POPG/PA, DPPC/POPC/PA and DPPC/PA membranes containing 0.57 mol% KL_4

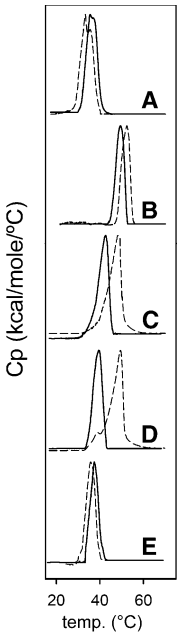

Fig. 3. Effect of calcium on the differential scanning calorimetry (DSC) heating scans of (A) DPPC/POPG, (B) DPPC/PA, (C) DPPC/POPC/PA and (D) DPPC/POPG/PA vesicles containing 0.57 mol% KL_4, and of (E) human lung surfactant isolated from healthy subjects. Calorimetric scans were performed at a rate of 0.5 °C·min^{-1} in the absence (broken line) or presence (unbroken line) of 1.8 mM $CaCl_2$. DPPC, 1,2-dipalmitoyl-phosphatidylcholine; PA, palmitic acid; POPC, 1-palmitoyl-2-oleoyl-phosphatidylcholine; POPG, 1-palmitoyl-2-oleoyl-phosphatidylglycerol.

(data not shown). This calcium-dependent T_m decrease was independent of the presence of KL_4 in the vesicles, as it was also observed in PA-containing vesicles without KL_4 (data not shown). These results are consistent with those of Henshaw and co-workers [27], who suggested that the calcium-dependent attenuation of PA-induced alterations of bilayer properties probably involved the extraction of PA from the bilayer at concentrations of > 100 μM calcium. Thus, the formation of PA–Ca^{2+} complexes might explain the decrease of the T_m of PA-containing vesicles induced by Ca^{2+}.

Figure 3 also shows calcium effects on the thermotropic properties of human lung surfactant isolated from healthy subjects (Fig. 3E). The thermogram obtained from human lung surfactant was characterized by a thermal transition showing the end of the melting process above 41 °C and a T_m of 37.2 ± 0.1 °C in the presence of calcium, which shifted slightly downward (36.2 ± 0.1 °C) in its absence. These data suggest that gel and fluid phases may coexist at physiological temperatures in surfactant membranes from human lungs. Lateral phase separation in natural surfactant from pig lungs was recently shown at 25 °C, a temperature below its T_m [28], and this phenomenon was independent of the presence of surfactant proteins [28]. The fact that the end of the melting process occurs at 41 °C, indicates that at this temperature (for instant, under high-fever conditions) surfactant membranes would be in the fluid state. The T_m of KL_4-DPPC/POPG/PA (39.5 ± 0.1 °C) was quite similar to the T_m of human lung surfactant in the presence of calcium and showed the end of the melting process at 41–42 °C. This suggests the fitness of this synthetic surfactant based on KL_4.

Effect of calcium and/or KL_4 on lipid lateral organization of surfactant-like membranes

To gain insight into the effects of calcium and/or KL_4 on the lipid lateral organization of surfactant-like membranes, confocal fluorescence microscopy of GUVs was employed. GUVs were prepared from DPPC/POPG, DPPC/POPC, DPPC/POPG/PA and DPPC/POPC/PA multilamellar vesicles doped with the fluorescent probe 2-(4,4-difluoro-5,7-dimethyl-4-bora-3α,4α-diaza-*s*-indacene-3-pentanoyl)-1-hexadecanoyl-*sn*-glycero-3-phosphocholine (Bodipy-PC) (Fig. 4). These 'cell size' vesicles (the average diameter was 21–25 μm) permit the direct visualization of lipid domain formation. POPG and/or PA-containing vesicles showed coexisting bright and dark domains at room temperature, well below their T_m. As Bodipy-PC partitions in the fluid phase [29], dark regions can be ascribed to DPPC-rich solid domains. Figure 4 shows that the number of DPPC solid domains is very low in DPPC/POPG GUVs in the absence of calcium, indicating a high level of miscibility between DPPC and POPG in these bilayers. Comparison of GUVs prepared from DPPC/POPG and DPPC/POPG/PA in the absence of Ca^{2+} indicated that adding PA to binary lipid mixtures of DPPC/POPG led to a considerable increase in the number and size of solid domains. These results are consistent with DPH anisotropy and DSC measurements reported above (Figs 1 and 2, respectively). Furthermore, Fig. 4 shows that the addition of Ca^{2+} to GUVs of DPPC/POPG increased the number of solid domains, while the addition of Ca^{2+} to DPPC/POPG/PA vesicles led to a marked decrease of the DPPC-rich solid domain fraction. These results are consistent with the calcium-dependent decrease of T_m by 10 °C determined by DSC measurements (Fig. 3) and can be explained by the partial extraction of PA from the membrane. The different lipid lateral organization in DPPC/POPG and DPPC/POPG/PA in the presence of Ca^{2+} strongly suggests that PA must not be totally extracted from the bilayer. Figure 4 also

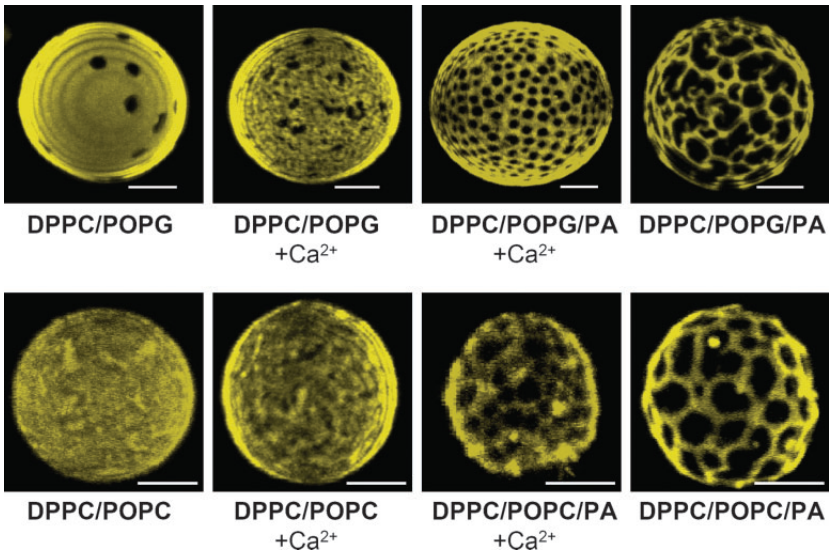

Fig. 4. Ca^{2+} effects on the lipid lateral organization of giant unilamellar vesicles (GUVs) prepared from DPPC/POPG and DPPC/POPG/PA (upper panel), and DPPC/POPC and DPPC/POPC/PA (lower panel) multilamellar vesicles doped with the fluorescent probe, 2-(4,4-difluoro-5,7-dimethyl-4-bora-3α,4α-diaza-*s*-indacene-3-pentanoyl)-1-hexadecanoyl-*sn*-glycero-3-phosphocholine (Bodipy-PC). Images were taken at 25 °C. The scale bars correspond to 5 μm. DPPC, 1,2-dipalmitoyl-phosphatidylcholine; PA, palmitic acid; POPC, 1-palmitoyl-2-oleoyl-phosphatidylcholine; POPG, 1-palmitoyl-2-oleoyl-phosphatidylglycerol.

shows that DPPC/POPC/PA, but not DPPC/POPC, giant vesicles showed the co-existence of gel/fluid phases at room temperature, and that the addition of Ca^{2+} resulted in a visible decrease of the solid domain fraction.

Figure 5 shows KL_4 effects on the lipid lateral organization of GUVs prepared from surfactant-like lipids in the absence and presence of Ca^{2+}. The yield of individual GUVs was very low in the presence of KL_4, and the GUVs formed displayed a smaller diameter (the average diameter was 11 μm) than in the absence of the peptide. Aggregates of vesicles could be visualized, indicating that the peptide induced vesicle aggregation. Figure 5 shows that the incorporation of KL_4 in either DPPC/POPG/PA or DPPC/POPC/PA giant vesicles induced changes in the shape and size of the solid domains. It is likely that the electrostatic interaction of KL_4 with POPG and/or PA would decrease the electrostatic repulsion between charged lipids and the miscibility between these lipids and DPPC, stabilizing DPPC-rich assemblies. The addition of calcium to DPPC/POPG/PA or DPPC/POPC/PA

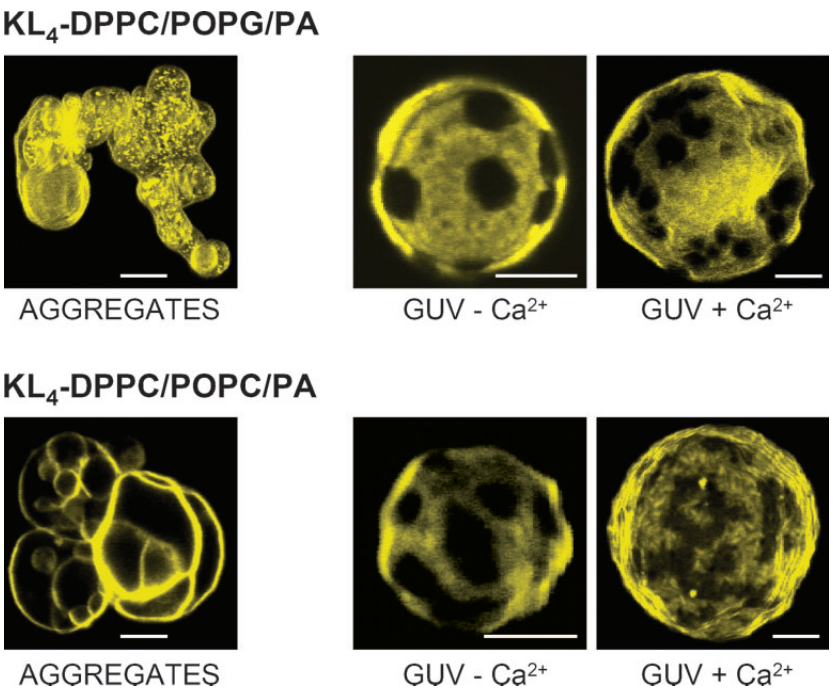

Fig. 5. KL_4 (0.57 mol%) effects on the lipid lateral organization of giant unilamellar vesicles (GUVs) prepared from DPPC/POPG/PA (upper panel) and DPPC/POPC/PA (lower panel) lipids in the absence and presence of Ca^{2+}. Images were taken at 25 °C. All the GUVs in the figure were labeled with the lipophilic fluorescence probe, 2-(4,4-difluoro-5,7-dimethyl-4-bora-3α,4α-diaza-*s*-indacene-3-pentanoyl)-1-hexadecanoyl-*sn*-glycero-3-phosphocholine (Bodipy-PC). The scale bars correspond to 5 μm. Fluorescence images of vesicle aggregation induced by KL_4 are also shown. DPPC, 1,2-dipalmitoyl-phosphatidylcholine; PA, palmitic acid; POPC, 1-palmitoyl-2-oleoyl-phosphatidylcholine; POPG, 1-palmitoyl-2-oleoyl-phosphatidylglycerol.

samples containing KL_4 reduced the DPPC-rich solid domain fraction, which is consistent with the calcium-dependent extraction of PA and the consequent decrease of T_m (Fig. 3). Importantly, these DPPC/POPG/PA or DPPC/POPC/PA vesicles containing KL_4 showed the co-existence of solid/fluid phases at room temperature, well below their T_m.

Effect of the lipid composition on KL_4 secondary structure and its dependence of calcium

The studies on KL_4 peptide available to date are not conclusive with regard to the secondary structure of the peptide in phospholipid membranes typically used in synthetic lung surfactant replacement. Cochrane & Revak [10] suggested that KL_4 in DPPC/PG mixed monolayers lies in the nonaqueous region and that the strong electrostatic forces between lysine residues and the anionic headgroup of phosphatidylglycerol dictate that the lysines would anchor along the charged polar headgroups, whereas the leucine side chains would penetrate the hydrophobic regions. The peptide would adopt a conformation with its backbone parallel to the interface. It would be possible for the peptide to display a random coil that might even take on some characteristics of a beta sheet or alpha helix. Fig. 6 shows that at low KL_4 concentrations (0.57 mol%), typically used in surfactant replacement for the clinical treatment of human RDS, KL_4 exhibited CD features consistent with an α-helical conformation in all vesicles that contained bilayer-fluidizing unsaturated phospholipids (i.e. POPG or POPC). These CD spectra were

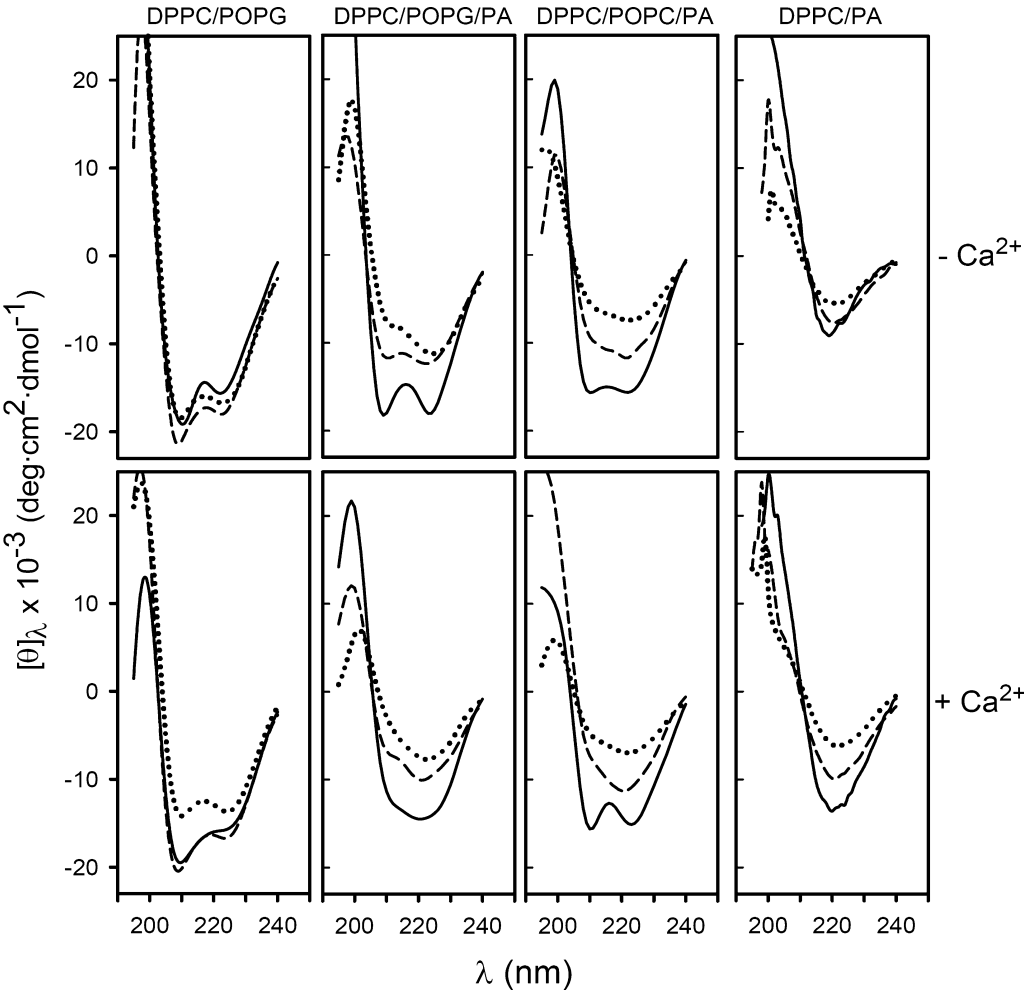

Fig. 6. CD spectra of KL_4 incorporated in DPPC/POPG, DPPC/POPG/PA, DPPC/POPC/PA and DPPC/PA membranes in the absence and presence of 1.8 mM $CaCl_2$. The following mol percentage concentrations of KL_4 were used: 0.57 (unbroken line), 1.2 (broken line) and 1.8 (dotted line). DPPC, 1,2-dipalmitoyl-phosphatidylcholine; PA, palmitic acid; POPC, 1-palmitoyl-2-oleoyl-phosphatidylcholine; POPG, 1-palmitoyl-2-oleoyl-phosphatidylglycerol.

characterized by two ellipticity minima at 208 and 222 nm and a marked maximum at 195 nm, as shown in Fig. 6. In contrast, KL_4 adopted a predominantly β-sheet structure, characterized by an ellipticity minimum at 220 nm and a maximum at 198 nm, in the vesicles lacking a membrane-fluidizing unsaturated lipid, specifically DPPC/PA. This indicates that the secondary structure of the peptide in surfactant-like membranes strongly depends on the presence of unsaturated phospholipids (either POPG or POPC) and therefore on membrane fluidity.

We have also studied calcium effects on the secondary structure of KL_4 inserted in these vesicles. Figure 6 (lower panel) shows that the addition of 1.8 mM Ca^{2+} did not substantially alter the KL_4 secondary structure. That is, KL_4 at low concentrations (0.57 mol%) retained its α-helical structure in the presence of calcium in the POPG or POPC-containing vesicles. In DPPC/PA vesicles; however, KL_4 adopted a predominantly β-sheet structure.

On the other hand, we found that α-helix to β-sheet transition takes place in DPPC/POPG/PA and DPPC/POPC/PA membranes, but not in DPPC/POPG membranes, as a consequence of the peptide/lipid concentration increase. This transition was more apparent in the presence of Ca^{2+}, especially in DPPC/POPC/PA vesicles (Fig. 6). The α-helical structure of KL_4 in these vesicles seems to be favored by electrostatic interactions between the positively charged lysine residues and negatively charged lipids (POPG and/or PA). Considering that the α-helical structure of KL_4 in DPPC/POPC/PA vesicles might be favored by electrostatic interactions between the charged lysine residues and ionized PA, it is conceivable that calcium could partly inhibit this interaction as a result of the partial extraction of PA from the membrane.

Our results agree with those of Cai *et al.* [16] and Gustafsson *et al.* [17], who studied the secondary structure of relatively high concentrations of KL_4 incorporated in monolayers or bilayers in the absence of Ca^{2+}. Cai and co-workers showed that 2.5–5 mol% KL_4 adopted an antiparallel β-sheet structure in DPPC and DPPC/DPPG (7 : 3, mol ratio) monolayers [16], whereas Gustafsson *et al.* found that 2.5 mol% KL_4 adopted an α-helix in DPPC/unsaturated-PG (7 : 3, w/w) bilayers [17]. In summary, our results supplemented by those published previously [16,17] permit the conclusion that the α-helical structure of KL_4 incorporated in membranes requires both neutralization of the positive charges of KL_4 with the negative charge of membrane lipids and the presence of unsaturated phospholipids, which decrease bilayer packing density. KL_4 α↔β transition takes place in membranes exhibiting solid/fluid phase co-existence, such as those of DPPC/POPG/PA or DPPC/POPC/PA, as the concentration of the peptide increased. This is favored by the presence of Ca^{2+}, which caused surface charge neutralization and/or PA extraction.

Role of the lipid composition and peptide structure on surface adsorption activity

Figure 7 shows the ability of different surfactant-like vesicles (DPPC/POPG, DPPC/POPG/PA, DPPC/POPC/PA and DPPC/PA) with and without different amounts of KL_4 to adsorb onto and spread at an air–water interface in the presence of physiological Ca^{2+}

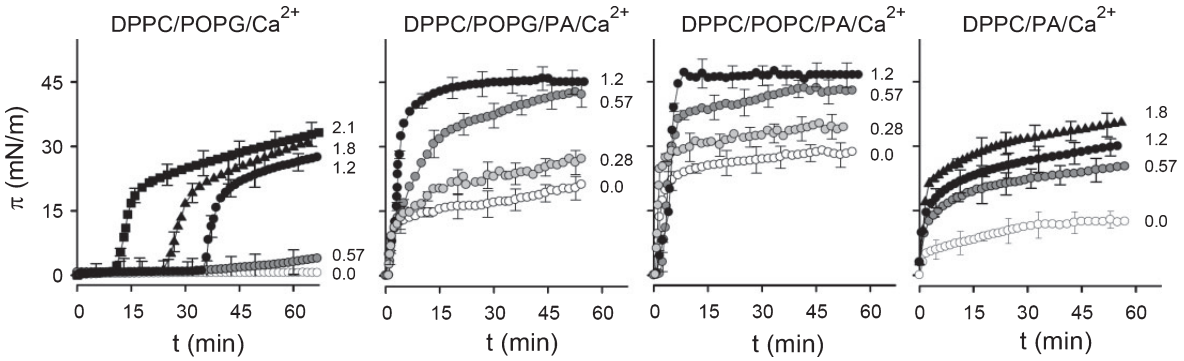

Fig. 7. Effect of different concentrations of KL_4 on the interfacial adsorption kinetics of DPPC/POPG, DPPC/POPG/PA, DPPC/POPC/PA and DPPC/PA membranes in the presence of calcium. Phospholipid interfacial adsorption was measured as a function of time for samples containing 70 μg·mL^{-1} of phospholipids in the absence (○) and presence of 0.28 mol% (●), 0.57 mol% (●), 1.2 mol% (●), 1.8 mol% (▲), and 2.1 mol% (■) KL_4 in a final volume of 6 mL of 5 mM Hepes buffer, pH 7.0, containing 150 mM NaCl and 1.8 mM $CaCl_2$. Similar results were found in the presence of 5 mM $CaCl_2$. DPPC, 1,2-dipalmitoyl-phosphatidylcholine; PA, palmitic acid; POPC, 1-palmitoyl-2-oleoyl-phosphatidylcholine; POPG, 1-palmitoyl-2-oleoyl-phosphatidylglycerol.

concentrations. Adsorption is carried out through (a) the transport of the material injected through the bulk liquid to the air/liquid interface and (b) the spreading of the material along the surface, which involved conversion from bilayer aggregates to interfacial film [30]. An inefficient surfactant adsorption would lead to a slower increase in surface pressure and the need for greater compression to attain the nearly zero surface tensions required for appropriate lung function. Synthetic replacement surfactants must adsorb quickly to a clean interface in a concentration-dependent manner up to the equilibrium surface pressure, π_e (40–45 $mN{\cdot}m^{-1}$) [7].

Figure 7 shows that, in the absence of the peptide, the vesicles (final phospholipid concentration of 70 $\mu g{\cdot}mL^{-1}$) showed no or very slow adsorption rates and neither system attained the equilibrium pressure, π_e, even with prolonged adsorption times. The presence of KL_4 improved the adsorption rate of all these liposomes, which increased with increasing mol% KL_4. Results also indicate that lipid composition plays a critical role in the surface activity of KL_4-surfactant preparations. Both KL_4-DPPC/POPG and KL_4-DPPC/PA surfactants showed slow adsorption rates and did not achieve the equilibrium pressure, even in the presence of high mol% KL_4. In contrast, for KL_4-DPPC/POPG/PA and KL_4-DPPC/POPC/PA surfactants containing KL_4 concentrations of ≥ 0.57 mol%, the surface pressure rose exponentially up to π_e. Concentrations of KL_4 higher than 1.2 mol% had no further effect on surface adsorption rate. Therefore, KL_4-DPPC/POPG/PA and KL_4-DPPC/POPC/PA surfactants were markedly superior to KL_4-DPPC/POPG surfactant (more fluid) and KL_4-DPPC/PA surfactant (excessively rigid) in their ability to adsorb rapidly onto and spread at an air–water interface. These results indicated that the presence of PA in surfactant-like membranes was decisive for rapid surface adsorption induced by KL_4 and that the replacement of the anionic POPG by the zwitterionic phospholipid POPC did not affect the surface activity of KL_4-surfactant. The common denominator of DPPC/POPG/PA and DPPC/POPC/PA vesicles, with and without KL_4, was that these membranes exhibited similar lipid lateral organization with co-existing fluid and solid phases, both in the absence and presence of calcium (Figs 4 and 5).

On the other hand, our results indicated that the conformational flexibility of the peptide (α-helical to β-sheet) did not affect the surface adsorption activity of KL_4-containing liposomes. These results suggest that the presence of α-helices is not critical for the surface activity of KL_4 peptide. They also corroborate previous findings of Castano and co-workers [31], who indicated that a predominantly α-helical structure is not essential for the surface activity of proteins or peptides containing alternating charged and hydrophobic residues.

The mechanism by which KL_4 peptide, or the surfactant proteins SP-B and SP-C, promote the rapid adsorption of surfactant-like vesicles to an air/water interface is not understood. The fusion of vesicle aggregates to the air/water interface must imply bilayer disruption. Energy must be supplied first to overcome hydration repulsion between membranes that approach each other and, second, to disrupt the normal bilayer structure of the fusing membranes. We show here that KL_4 induces vesicle aggregation (Fig. 5). This might facilitate the build-up of a multilayered surface-associated surfactant reservoir. In addition, KL_4 might act synergistically with Ca^{2+} to cause charge neutralization

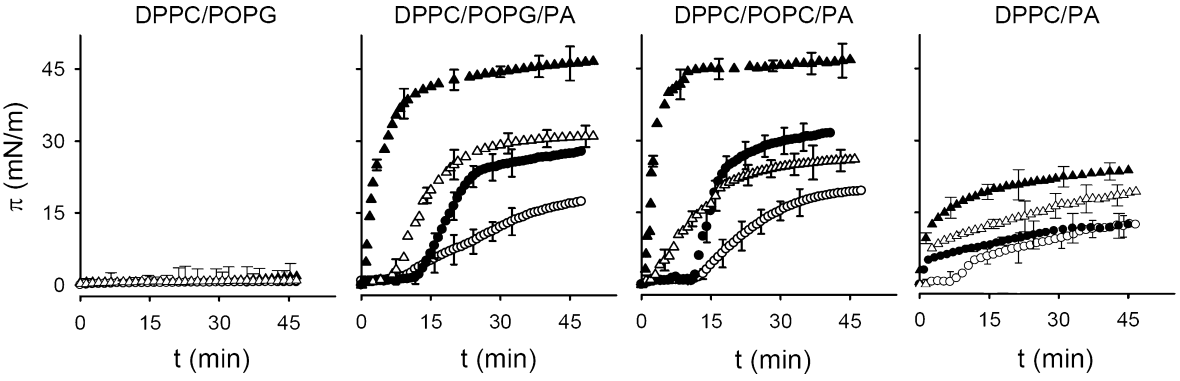

Fig. 8. Effect of KL_4 on the interfacial adsorption kinetics of DPPC/POPG, DPPC/POPG/PA, DPPC/POPC/PA, and DPPC/PA membranes in the absence of $CaCl_2$. Phospholipid interfacial adsorption was measured as a function of time for samples containing 70 $\mu g{\cdot}mL^{-1}$ (circles) or 160 $\mu g{\cdot}mL^{-1}$ of phospholipid (triangles) in the absence (white symbols) and presence (black symbols) of 0.57 mol% KL_4 in a final volume of 6 mL of 5 mM Hepes buffer, pH 7.0, containing 150 mM NaCl. DPPC, 1,2-dipalmitoyl-phosphatidylcholine; PA, palmitic acid; POPC, 1-palmitoyl-2-oleoyl-phosphatidylcholine; POPG, 1-palmitoyl-2-oleoyl-phosphatidylglycerol.

and local dehydration of contacting surfaces containing POPG/PA- or POPC/PA-rich domains. Adsorption experiments performed in the absence of calcium (Fig. 8) indicate that KL_4-containing DPPC/POPG/PA or DPPC/POPC/PA membranes (final phospholipid concentration of 70 $\mu g \cdot mL^{-1}$) showed very slow adsorption rates and did not reach the equilibrium surface pressure. It was necessary to raise the amount of lipid in samples containing 0.57 mol% KL_4 to 160 $\mu g \cdot mL^{-1}$ to achieve π_e (Fig. 8). These results indicate that KL_4 and Ca^{2+} seem to act synergistically in the surface adsorption process. We speculate that in the presence of KL_4 and/or Ca^{2+}, the unsaturated phospholipids, POPC and POPG, might form transient, negatively curved structures in the bilayer–monolayer transition [32,33] or rapidly flip to the air–water interface.

Conclusions

In summary, we report that both the membrane lipid composition and the presence of calcium affected the KL_4 structure. The secondary structures adopted by the peptide are a function of (a) the negative charge on the membrane surface, which in turn depends on the presence of calcium, (b) the bilayer packing density, and (c) the concentration of the peptide in the membrane. We found that KL_4 adopted a predominantly α-helical secondary structure in DPPC/POPG vesicles and a predominantly β-sheet structure in DPPC/PA vesicles, independently of the presence of calcium and at different peptide mole percentages (0.57–1.8 mol%). However, in DPPC/POPG/PA or DPPC/POPC/PA liposomes, KL_4 interconverted to a β-sheet structure as the concentration of the peptide increased. This process was favored in the presence of Ca^{2+}. KL_4 α↔β conformational flexibility did not influence the surface adsorption activity of KL_4-containing vesicles. We suggest that the KL_4 concentration-dependent ordering effect on POPG and POPC-containing membranes and the peptide's ability to induce vesicle aggregation are related to its surface activity.

With respect to the lipid component of KL_4-containing synthetic surfactants, we found that the physical state of the membrane plays a critical role in the surface adsorption process. Thus, KL_4-containing DPPC/POPG/PA and DPPC/POPC/PA vesicles, which showed well-defined solid/fluid phase co-existence at temperatures below their T_m, exhibited very rapid surface adsorption, even in the absence of calcium. In contrast, more fluid (DPPC/POPG) or excessively rigid (DPPC/PA) KL_4-containing membranes fail in their ability to rapidly adsorb onto an air–water interface. The presence of PA in either DPPC/POPG or DPPC/POPC membranes containing KL_4 was important as PA leads to the lateral redistribution of lipids, increasing the fraction of DPPC-rich solid domains, which results in phase separation. Several studies indicate that phase separation exists in natural surfactant [28] and in membranes from lipid extracts of surfactant [34] at physiological temperatures. Together, these findings suggest that phase co-existence in synthetic surfactants at physiological temperatures might be important for them to function adequately.

One disadvantage of surfactant-like mixtures containing PA is that the T_m of these vesicles is very high. However, we found that calcium markedly decreased the T_m of PA-containing vesicles. Thus, in the presence of physiological concentrations of calcium, the T_m value of KL_4-containing DPPC/POPG/PA membranes shifted from 48.3 to 39.5 °C. This T_m value was quite similar to that of human lung surfactant membranes isolated from healthy subjects (37.2 °C), and both systems showed the end of the melting process at 41 °C. The decrease of the T_m in PA-containing vesicles is explained by the partial extraction of PA from the bilayer by the formation of PA/Ca^{2+} complexes. The different T_m and lipid lateral organization in DPPC/POPG and DPPC/POPG/PA vesicles in the presence of Ca^{2+} clearly indicated that PA was just partly extracted from the bilayer. These results suggest that the amount of PA needed to increase the fraction of DPPC-rich solid domains and improve the *in vitro* surface activity of synthetic surfactants is much smaller than that previously proposed [19]. Hence, the results reported here might be useful for designing new lipid mixtures for replacement surfactants containing synthetic or recombinant peptides with optimal surface activity.

Experimental procedures

Materials

Synthetic lipids, DPPC, POPG, POPC, and PA were purchased from Avanti Polar Lipids (Birmingham, AL, USA). The organic solvents (methanol and chloroform) used to dissolve the lipids were HPLC-grade (Scharlau, Barcelona, Spain). Bodipy-PC and DPH were purchased from Molecular Probes (Eugene, OR, USA). All other reagents were of analytical grade and obtained from Merck (Darmstadt, Germany).

Vesicles of DPPC/POPG (27 : 9, w/w), DPPC/POPG/PA (28 : 9.4 : 5.1, w/w/w), DPPC/POPC/PA (28 : 9.4 : 5.1, w/w/w) and DPPC/PA (28 : 5.1, w/w), with different amounts of KL_4 peptide, were prepared as previously reported [35,36]. The sample solutions were prepared by mixed

stock solution of the lipid and the peptide, both prepared in chloroform/methanol, to achieve the desired lipid/peptide ratio. Human lung surfactant was isolated and characterized as described previously [37].

Emission anisotropy measurements

Steady-state fluorescence emission anisotropy measurements were carried out using an SLM-Aminco AB2 spectrofluorimeter equipped with Glam prism polarizers and a thermostated cuvette holder (Thermo Spectronic, Waltham, MA, USA) (± 0.1 °C), using 5×5 mm path-length quartz cuvettes. The required amounts of KL_4 surfactant were mixed with DPH at a probe/phospholipid molar ratio of 1 : 200 (final phospholipid concentration of 1 mg·mL^{-1}), as previously described [35]. Excitation and emission wavelengths were set at 360 and 430 nm, respectively. For each sample, fluorescence emission intensity data in parallel and perpendicular orientations, with respect to the exciting beam, were collected 10 times each and then averaged. Background intensities in DPH-free samples as a result of the vesicles were subtracted from each recording of fluorescence intensity. Anisotropy, r, was calculated as:

$$r = \frac{I_{\parallel} - G \cdot I_{\perp}}{I_{\parallel} + 2G \cdot I_{\perp}}$$

where $I_{\parallel}$ and $I_{\perp}$ are the parallel and perpendicular polarized intensities measured with the vertically polarized excitation light and G is the monochromator grating correction factor.

DSC

Calorimetric measurements were performed as previously reported [35] in a Microcal VP DSC (Microcal Inc., Northampton, MA, USA) at a heating rate of 0.5 °C·min^{-1}. Surfactant-like multilamellar vesicles (1 mM), in the absence and presence of different amounts of KL_4, were loaded in the sample cell of the microcalorimeter with buffer (130 mM NaCl, 20 mM Tris/HCl, pH 7.6, either with or without 1.8 mM $CaCl_2$) in the reference cell. Three calorimetric scans were collected from each sample between 15 and 70 °C. For each preparation, the analysis was repeated two or three times. The standard MICROCAL ORIGIN software was used for data acquisition and analysis. The excess heat capacity functions were obtained after subtraction of the buffer–buffer baseline.

GUV

GUVs composed of DPPC/POPG, DPPC/POPC, DPPC/POPG/PA, or DPPC/POPC/PA, in the absence and presence of KL_4, were prepared from lipid samples suspended in buffer solution (no organic solvents), as described previously [28], by using the electroformation method [38]. Briefly, ≈3 μL of the stock suspension in buffer, labelled with Bodipy-PC, as reported previously [28], was spread on the surface of each platinum wire as small drops. The chamber was then placed under a stream of N_2 and subsequently under low vacuum for 30 min to allow the native material to adsorb onto the platinum wire. An important point in this step is to avoid dehydration of the sample to maintain the integrity of the membranes. Once the material was adsorbed to the platinum wire, aqueous solution was added to the chamber (200 mosM sucrose solution prepared with Millipore-filtered water, 17.5 megohms·cm^{-1}). The sucrose solution was previously heated to the desired temperature (above the lipid mixture phase transition), and then sufficient volume was added to cover the platinum wires (≈ 300 μL). The platinum wires were connected immediately to a function generator (Digimess® FG 100, Vann Draper electronics Ltd., Derby, UK), and a low-frequency AC field (sinusoidal wave function with a frequency of 10 Hz and an amplitude of 3 V) was applied for 60 min. After vesicle formation, the AC field was turned off, and the vesicles were collected with a pipette and transferred to a plastic tube.

Observation of giant vesicles

Aliquots of giant vesicles suspended in sucrose were added to an equi-osmolar concentration of glucose solution. Because of the density difference between the two solutions, the vesicles precipitate at the bottom of the chamber, which facilitates observation of the GUVs in the inverted confocal microscope. GUV preparations were observed in 12-well plastic chambers (Laboratory-Tek Brand Products, Naperville, IL, USA). The chamber was located in an inverted confocal microscope (Zeiss LSM 510 META, Zeiss, Jena, Germany) for observation. The excitation wavelength was 488 nm for Bodipy-PC. The temperature was controlled from a water bath connected to a homemade device into which the 12-well plastic chamber was inserted. The temperature was measured inside the sample chamber using a digital thermocouple (model 400B; Omega Inc., Stamford, CT, USA) with a precision of 0.1 °C. Unilamellarity was assured by measuring the fluorescence intensity of the equator region, as previously described [39].

CD measurements

CD spectra of surfactant-like vesicles (final phospholipid concentration of 800 μg·mL^{-1}) containing different amounts of KL_4 were obtained on a Jasco J-715 spectropolarimeter fitted with a 150-watt xenon lamp as previously performed with surfactant proteins SP-A, SP-B, and SP-C [36,40,41]. Quartz cells of 1 mm path-length were used. Four scans were accumulated and averaged for each spectrum. The acquired spectra were corrected by subtracting the appropriate blank runs of phospholipid vesicle solutions, subjec-

ted to noise reduction analysis, and presented as molar ellipticities (deg·cm^2·dmol^{-1}). All measurements were performed in 130 mM NaCl, 20 mM Tris/HCl buffer, pH 7.6, at 25 °C, in the absence or presence of either 1.8 mM or 5 mM $CaCl_2$. For each preparation, the analysis was repeated at least three times. Estimation of the secondary structure content from the CD spectra was performed after deconvolution of the spectra into four simple components (α-helix, β-sheet, β-turns, and random coil), according to the convex constraint algorithm [42].

Adsorption assays

The ability of the lipid mixtures to absorb onto and spread at the air–water interface was tested in the absence and presence of KL_4, at 25 and 37 °C, in a Wilhelmy-like high sensitive surface microbalance [36,43]. The samples were injected into the hypophase chamber of the Teflon dish, which contained 6 mL of 5 mM Hepes buffer, pH 7.0, 150 mM NaCl, either with or without 5 mM $CaCl_2$, with continuous stirring. Interfacial adsorption was measured following the change in surface tension as a function of time. For each preparation, the analysis was repeated at least three times.

Acknowledgements

This work was supported by Fondo de Investigación Sanitaria 03/0137 and by Dr Esteve, S.A. Laboratorios (Barcelona). Research in the laboratory of L. A. B. is funded by a grant from SNF, Denmark (21-03-0569) and the Danish National Research Foundation (which supports MEMPHYS-Center for Biomembrane Physics). We acknowledge Dr Charles Cochrane, from the Scripps Research Institute (La Jolla, CA 92037), for his useful suggestions on a critical reading of the manuscript.

References

1 Goerke J (1998) Pulmonary surfactant: functions and molecular composition. *Biochim Biophys Acta* **1408**, 79–89.
2 Piknova B, Schram V & Hall S (2002) Pulmonary surfactant: phase behaviour and function. *Curr Opin Struct Biol* **21**, 487–494.
3 Whitsett JA & Weaver TE (2002) Hydrophobic surfactant proteins in lung function and disease. *N Engl J Med* **347**, 2141–2148.
4 Wright JR (2005) Immunomodulatory functions of surfactant proteins. *Nat Rev Immunol* **5**, 58–68.
5 Veldhuizen EJ, Nag K, Orgeig S & Possmayer F (1998) The role of lipids in pulmonary surfactant. *Biochim Biophys Acta* **1408**, 90–108.
6 Robertson B & Halliday HL (1998) Principles of surfactant replacement. *Biochim Biophys Acta* **1408**, 346–361.
7 Robertson B, Johansson J & Curstedt T (2000) Synthetic surfactants to treat neonatal lung disease. *Mol Med Today* **6**, 119–124.
8 Revak SD, Merritt TA, Degryse E, Stefani L, Courtney M, Hallman M & Cochrane CG (1988) Use of human surfactant low molecular weight apoproteins in the reconstitution of surfactant biologic activity. *J Clin Invest* **81**, 826–833.
9 Waring A, Taeusch W, Bruni R, Amirkhanian J, Fan B, Stevens R & Young J (1989) Synthetic amphipathic sequences of surfactant protein-B mimic several physicochemical and *in vivo* properties of native pulmonary surfactant proteins. *Pept Res* **2**, 308–313.
10 Cochrane CG & Revak SD (1991) Pulmonary surfactant protein B (SP-B): structure–function relationships. *Science* **254**, 566–568.
11 Cochrane CG, Revak SD, Merritt TA, Heldt GP, Hallman M, Cunningham MD, Easa D, Pramanik A, Edwards DK & Alberts MS (1996) The efficacy and safety of KL4-surfactant in preterm infants with respiratory distress syndrome. *Am J Respir Crit Care Med* **153**, 404–410.
12 Sinha SK, Lacaze-Masmonteil T, Valls i Soler A, Wiswell TE, Gadzinowski J, Hajdu J, Bernstein G, Sanchez-Luna M, Segal R, Schaber CJ *et al.* (2005) Surfaxin Therapy Against Respiratory Distress Syndrome Collaborative Group. A multicenter, randomized, controlled trial of lucinactant versus poractant alfa among very premature infants at high risk for respiratory distress syndrome. *Pediatrics* **115**, 1030–1038.
13 Cochrane CG, Revak SD, Merritt TA, Schraufstatter IU, Hoch RC, Henderson C, Andersson S, Takamori H & Oades ZG (1998) Bronchoalveolar lavage with KL4-surfactant in models of meconium aspiration syndrome. *Pediatr Res* **44**, 705–715.
14 Wiswell TE, Smith RM, Katz LB, Mastroianni L, Wong DY, Willms D, Heard S, Wilson M, Hite RD, Anzueto A *et al.* (1999) Bronchopulmonary segmental lavage with surfaxin (KL_4-surfactant) for acute respiratory distress syndrome. *Am J Respir Crit Care Med* **160**, 1188–1195.
15 Ma J, Koppenol S, Yu H & Zografi G (1998) Effects of a cationic and hydrophobic peptide, KL4, on model lung surfactant lipid monolayers. *Biophys J* **74**, 1899–1907.
16 Cai P, Flach CR & Mendelsohn R (2003) An infrared reflection-absorption spectroscopy study of the secondary structure in KL_4, a therapeutic agent for respiratory distress syndrome, in aqueous monolayers with phospholipids. *Biochemistry* **42**, 9446–9452.
17 Gustafsson M, Vandenbussche G, Curstedt T, Ruysschaert JM & Johansson J (1996) The 21-residue surfactant peptide $(LysLeu)_4Lys$ (KL4) is a transmembrane

α-helix with a mixed nonpolar/polar surface. *FEBS Lett* **384**, 185–188.
18 Nilsson G, Gustafsson M, Vandenbussche G, Veldhuizen E, Griffiths WJ, Sjövall J, Haagsman HP, Ruysschaert JM, Robertson B, Curstedt T *et al.* (1998) Synthetic peptide-containing surfactants. Evaluation of transmembrane versus amphipathic helices and surfactant protein C poly-valyl and poly-leucyl substitution. *Eur J Biochem* **255**, 116–124.
19 Tanaka Y, Takei T, Aiba T, Masuda K, Kiuchi A & Fujiwara T (1986) Development of synthetic lung surfactants. *J Lipid Res* **27**, 475–485.
20 Johansson J, Some M, Linderholm BM, Almlen A, Curstedt T & Robertson B (2003) A synthetic surfactant based on a poly-Leu SP-C analog and phospholipids: effects on tidal volumes and lung gas volumes in ventilated immature newborn rabbits. *J Appl Physiol* **95**, 2055–2063.
21 Lentz BR (1989) Membrane 'fluidity' as detected by diphenylhexatrien probes. *Chem Phys Lipids* **50**, 171–190.
22 Lakowicz JR (1999) *Principles of Fluorescence Spectroscopy*, 2nd edn. Kluwer Academic/Plenum Publishers, New York.
23 Baatz JE, Sarin V, Absolom DR, Baxter C & Whitsett JA (1991) Effects of surfactant-associated protein SP-B synthetic analogs on the structure and surface activity of model membrane bilayers. *Chem Phys Lipids* **60**, 163–178.
24 Vincent JS, Revak SD, Cochrane CG & Levin IW (1991) Raman spectroscopic studies of model human pulmonary surfactant systems: phospholipid interactions with peptide paradigms for the surfactant protein SP-B. *Biochemistry* **30**, 8395–8401.
25 Piknova B, Schief WR, Vogel V, Discher BM & Hall SB (2001) Discrepancy between phase behavior of lung surfactant phospholipids and the classical model of surfactant function. *Biophys J* **81**, 2172–2180.
26 Nielson DW (1986) Electrolite composition of pulmonary alveolar subphase in anesthetized rabbits. *J Appl Physiol* **60**, 972–979.
27 Henshaw JB, Olsen CA, Farnbach AR, Nielson KH & Bell JD (1998) Definition of the specific roles of lysolecithin and palmitic acid in altering the susceptibility of dipalmitoylphosphatidylcholine bilayers to phospholipase A2. *Biochemistry* **37**, 10709–10721.
28 Bernardino de la Serna J, Perez-Gil J, Simonsen AC & Bagatolli LA (2004) Cholesterol rules: direct observation of the coexistence of two fluid phases in native pulmonary surfactant membranes at physiological temperatures. *J Biol Chem* **279**, 40715–40722.
29 Huang N, Florine-Casteel K, Feigenson GW & Spink C (1988) Effect of fluorophore linkage position of n-(9-anthroyloxy) fatty acids on probe distribution between coexisting gel and fluid phospholipid phases. *Biochim Biophys Acta* **939**, 124–130.
30 Walters RW, Jenq RR & Hall SB (2000) Distinct steps in the adsorption of pulmonary surfactant to an air–liquid interface. *Biophys J* **78**, 257–266.
31 Castano S, Desbat B, Laguerre M & Dufourcq J (1999) Structure, orientation and affinity for interfaces and lipids of ideally amphipathic lytic LiKj (i=2j) peptides. *Biochim Biophys Acta* **1416**, 176–194.
32 Schram V & Hall SB (2004) SP-B and SP-C alter diffusion in bilayers of pulmonary surfactant. *Biophys J* **86**, 3734–3743.
33 Biswas SC, Rananavare SB & Hall SB (2005) Effects of gramicidin-A on the adsorption of phospholipids to the air–water interface. *Biochim Biophys Acta* **1717**, 41–49.
34 Nag K, Pao JS, Harbottle RR, Possmayer F, Petersen NO & Bagatolli LA (2002) Segregation of saturated chain lipids in pulmonary surfactant films and bilayers. *Biophys J* **82**, 2041–2051.
35 Canadas O, Guerrero R, Garcia-Canero R, Orellana G, Menéndez M & Casals C (2004) Characterization of liposomal tacrolimus in lung surfactant-like phospholipids and evaluation of its immunosuppressive activity. *Biochemistry* **43**, 9926–9938.
36 Sanchez-Barbero F, Strassner J, Garcia-Canero R, Steinhilber W & Casals C (2005) Role of the degree of oligomerization in the structure and function of human surfactant protein A. *J Biol Chem* **280**, 7659–7670.
37 Casals C, Arias-Diaz J, Valiño F, Saenz A, Garcia C, Balibrea JA & Vara E (2003) Surfactant stregthens the inhibitory effect of C-reactive protein on human lung macrophage cytokine release. *Am J Physiol Lung Cell Mol Physiol* **284**, L466–L472.
38 Angelova MI & Dimitrov DS (1986) Liposome electroformation. *Faraday Discuss Chem Soc* **81**, 303–311.
39 Akashi K, Miyata H, Itoh H & Kinosita K Jr (1996) Preparation of giant liposomes in physiological conditions and their characterization under an optical microscope. *Biophys J* **71**, 3242–3250.
40 Ruano MLF, Perez-Gil J & Casals C (1998) Effect of acidic pH on the structure and lipid binding properties of porcine surfactant protein A. Potential role of acidification along its exocytic pathway. *J Biol Chem* **273**, 15183–15191.
41 Cruz A, Casals C & Perez-Gil J (1995) Conformational flexibility of pulmonary surfactant proteins SP-B and SP-C, studied in aqueous organic solvents. *Biochim Biophys Acta* **1255**, 68–76.
42 Perczel A, Park K & Fasman GD (1992) Analysis of the circular dichroism spectrum of proteins using the convex constraint algorithm: a practical guide. *Anal Biochem* **203**, 83–93.
43 Casals C, Varela A, Ruano MLF, Valiño F, Perez-Gil J, Torre N, Jorge E, Tendillo F & Castillo-Olivares JL (1998) Increase of C-reactive protein and decrease of surfactant protein A in surfactant alter lung transplantation. *Am J Respir Crit Care Med* **175**, 43–49.